https://doi.org/10.5194/acp-2022-579
Preprint. Discussion started: 6 September 2022

Atmospheric Chemistry and Physics Discussions

Quantifying daily NO_x and CO_2 emissions from Wuhan using satellite observations from TROPOMI and OCO-2

Qianqian Zhang[1,2], K. Folkert Boersma[1,3], Bin Zhao[4], Henk Eskes[3], Cuihong Chen[5], Haotian Zheng[4], Xingying Zhang[2]

[1] Wageningen University, Environmental Science Group, Wageningen, the Netherlands
[2] Key Laboratory of Radiometric Calibration and Validation for Environmental Satellites, Innovation Center for Fengyun Meteorological Satellite (FYSIC), National Satellite Meteorological Center, China Meteorology Administration, Beijing, 100081, China
[3] Royal Netherlands Meteorological Institute, De Bilt, the Netherlands
[4] State Key Joint Laboratory of Environmental Simulation and Pollution Control, School of environment, Tsinghua University, Beijing 100084, China
[5] Satellite Application Center for Ecology and Environment, Ministry of Ecology and Environment of the People's Republic of China, Beijing, 100094, China

Correspondence to: K. Folkert Boersma, folkert.boersma@wur.nl, Qianqian Zhang, zhangqq@cma.gov.cn

Abstract. Quantification and control of NO_x and CO_2 emissions are important across the world to limit adverse climate change. We present a new top-down method, an improved superposition column model to estimate day-to-day NO_x and CO_2 emissions from the large city of Wuhan, China, located in a polluted background. The lasted released version 2.3.1 TROPOMI NO_2 columns and the version 10r of the OCO-2 observed CO_2 mixing ratio are employed. Our estimated NO_x and CO_2 emissions from Wuhan are verified against bottom-up inventories with small deviations (< 3 %). Based on the estimated CO_2 emissions, we also predicted daily CO_2 column mixing ratio enhancements, which match well with OCO-2 observations (< 5 % bias, within ±0.3 ppm). We capture the day-to-day variation of NO_x and CO_2 emissions from Wuhan in 2019–2020, which does not reveal a substantial 'weekend reduction' but does show a clear 'holiday reduction' in the NO_x and CO_2 emissions. Our method also quantifies the abrupt decrease and slow rebound of NO_x and CO_2 emissions due to the Wuhan lockdown in early 2020. This work demonstrates the improved superposition model to be a promising new tool for the quantification of city NO_x and CO_2 emissions, allowing policy makers to gain real-time information into spatial-temporal emission patterns and the effectiveness of carbon and nitrogen regulation in urban environments.

https://doi.org/10.5194/acp-2022-579
Preprint. Discussion started: 6 September 2022

Atmospheric Chemistry and Physics Discussions

1 Introduction

Fossil fuel combustion by power plants, industrial activities, transportation, and residential energy use sectors leads to emission of nitrogen oxides (NO_x = NO + NO_2) as well as carbon dioxide (CO_2). Traditional bottom-up NO_x and CO_2 emission estimates have a lag in time of several years, because it takes time to access and compile accurate information on energy consumption and the emission factors (Lamsal et al., 2011; Liu et al., 2020a).

For decades satellites have been continuously providing information of NO_2 distributions and trends with good quality, and satellite data is widely used to quantify NO_x emissions and changes(Lamsal et al., 2010; Visser et al., 2019; Zhang et al., 2020; Zhang et al., 2021). Based on satellite retrieved NO_2 data, previous studies quantified long-term mean (monthly, yearly or multi-yearly) NO_x emissions on global and regional scales(Lamsal et al., 2011; Visser et al., 2019). Beirle et al. (2011) analyzed downwind plumes of satellite NO_2 columns averaged on each wind direction, and then inferred NO_x emissions from isolated large point sources and megacities. Inspired by this idea, Lorente et al. (2019) analyzed the increase of NO_2 along with the wind over the extensive pollution source of Paris. The build-up of NO_2 over the city observed from space, in combination with information on wind speed and direction allows to obtain day-by-day (sub-)urban NO_x emission estimates and lifetimes as long as the city is under a clear sky and winds are relatively constant in time. This approach does not need burdensome inverse modelling computations and opens possibilities for rapid and direct monitoring of NO_x emissions from space.

In contrast to NO_x, it is challenging to infer accurate localized anthropogenic CO_2 emissions from satellite CO_2 retrievals. One reason is that the background CO_2 concentration is orders of magnitude higher than the enhancement caused by anthropogenic emissions, reflecting the long atmospheric lifetime of CO_2 (Reuter et al., 2014; 2019). Another reason is that the spatial and temporal coverage of current CO_2 sensors is too sparse to allow substantial averaging of noisy signals by revisiting of scenes, precluding detailed CO_2 emission estimation(Zheng et al., 2020a; Liu et al., 2020a). Using satellite NO_2 measurements to estimate anthropogenic NO_x emissions as the basis to infer anthropogenic CO_2 emission has been proposed in several studies(Reuter et al., 2019; Liu et al., 2020a; Berezin et al., 2013; Zheng et al., 2020a). However, to our knowledge there is no method that estimates day-to-day top-down CO_2 emission estimation on (sub-)city scale.

Here we revisit the method of Lorente et al. (2019) to improve our understanding of its potential and limitations and extend it to estimate city-scale daily NO_x and CO_2 emissions. We present an improved superposition model that considers the build-up of pollution over a source area as in Lorente et al. (2019), as well as the decay of NO_2 downwind of the source, but now also accounts for changes in the background NO_2 pollution along wind direction. The background NO_2 pollution was considered to remain constant in Lorente et al. (2019) for Paris, which is not surrounded by significant surface sources of NO_x pollution. Here we apply our improved method on a highly polluted urban area, the megacity of Wuhan in Hubei Province of China, which, other than the relatively isolated city of Paris, is located in a polluted background with many surrounding surface pollution sources that potentially interfere with the build-up and decay of the NO_2 plume from Wuhan. Using this improved superposition model, together with the bottom-up information on CO_2-to-NO_x emission ratio, we infer

https://doi.org/10.5194/acp-2022-579
Preprint. Discussion started: 6 September 2022


Atmospheric Chemistry and Physics Discussions

NO_x and predict CO_2 emissions on a day-by-day basis over a full year, from September 2019 to August 2020, and analyze the variation in emissions and NO_x chemical lifetime from day to day. Of particular interest are the reductions and subsequent rebound of NO_x and CO_2 emissions associated with the COVID-19 lockdown measures in Wuhan, which have been reported in other studies, and serve here as a useful check on the robustness of our method.

2 Data and Material

2.1 Satellite data

In this study, we use the newly released level-2, version 2.3.1 of the S-5P TROPOMI data (TROPOMI-v2.3.1) between September 2019 to August 2020. The S-5P (Sentinel-5 Precursor) satellite was launched in October 2017, and the TROPOMI (TROPOspheric Monitoring Instrument) on board provides tropospheric NO_2 columns with a unprecedented horizontal resolution up to 5.5km × 3.5km (as of 6 August 2019) and high signal-to-noise ratio(Griffin et al., 2019; Van Geffen et al., 2020). The v2.3.1 dataset is provided by S5P-PAL (Eskes et al., 2021), and is dedicated to support the research on the impact of the COVID lockdown on air quality. Compared to the earlier version, this dataset has 10–40 % higher tropospheric NO_2 columns over polluted scenes due to the improved cloud retrieval and other algorithm updates (Van Geffen et al., 2022; Riess et al., 2022). Over Wuhan we find an average increase of about 25 %, but the difference between the two versions changes spatially and temporally (Fig. S2). According to Fig. S2, the increase in v2.3.1 is much higher over polluted area (city center) and polluted period (9 September and 3 October 2019). Improved (residual) cloud pressures correct the low bias of v1.x data compared to OMI and ground-based measurements over east China (Wang et al., 2020; Liu et al., 2020b). In addition, an improved treatment for the surface albedo increases the columns for cloud-free scenes (Van Geffen et al., 2022). For comparison (and to assess the impact of retrieval improvements on NO_x emission estimates), we also use version 1.3 data (TROPOMI-v1.3) for 2019 to derive NO_x emissions from Wuhan. Since previous studies have pointed out a low bias in the v1.x TROPOMI retrieval, especially over China (Griffin et al., 2019; Wang et al., 2020; Liu et al., 2020b), we scaled up the v1.3 NO_2 columns by a factor of 1.6 to correct for this known -40 % bias in TROPOMI NO_2 data as reported by Liu et al. (2020b).

We sampled the TROPOMI NO_2 columns into 0.05° lat × 0.05° lon grid cells (~ 6 × 6 km^2). To assure good data quality, we filtered out the data with cloud radiance fractions greater than 0.5 (qa_value > 0.75), and obtain 81 clear-sky days with full TROPOMI NO_2 coverage over the Wuhan region in one full year.

The column-averaged dry air mole fraction of CO_2 (XCO_2) data provided by the Orbiting Carbon Observatory-2 (OCO-2) are also employed to verify the derived CO_2 emission inventory for Wuhan. We use the version 10r of the bias-corrected XCO_2 product (Gunson M and Eldering, 2020). The v10 OCO-2 XCO_2 product has high accuracy with single sounding precision of ~0.8 ppm over land and ~0.5 ppm over water, and RMS biases of 0.5–0.7 ppm over both land and water (Odell et al., 2021).

https://doi.org/10.5194/acp-2022-579
Preprint. Discussion started: 6 September 2022


Atmospheric Chemistry and Physics Discussions

2.2 Bottom-up emission information

Bottom-up NO_x and CO_2 emission inventories are used to provide the first-guess of NO_x emission spatial pattern (for NO_x, in the Supplement, Text S1 and Fig. S1) and to verify the top-down emissions. We use the Air Benefit and Attainment and Cost Assessment System Emission Inventory (ABACAS) (Zhao et al., 2013; Zhao et al., 2018; Zheng et al., 2019) , which provides NO_x and CO_2 emissions for the year 2019. The Multi-resolution Emission Inventory (MEIC) (Li et al., 2017) NO_x emissions for 2017 are also used.

2.3 Other input data

Besides the satellite data and bottom-up emission inventories, a set of other parameters are used to input into our improved superposition model. They include the hydroxyl radical (OH) concentration, the loss rate (k) of NO_x in the atmosphere, the $[NO_x]/[NO_2]$ ratio, and the wind field. The first three are from the GEOS-Chem chemical transport model, and the wind field is from ERA5, the fifth generation ECMWF atmospheric reanalysis of the global climate (Hersbach et al., 2020). Detailed information of these data is seen in the supplement, Text S2.

2.4 NO_2 pattern fits: estimation of lifetime and emission

To ensure that the whole area of Wuhan is included, we determine our study domain as a circular region centered at 114° E, 30.7° N, with a diameter of ~186 km. It includes the whole area of Wuhan and the small city of Ezhou to the east of Wuhan, the southwest part of Huanggang and east part of Xiaogan (Fig. S3). We also do a sensitivity test to narrow the study area down to within the Third Ring Road of Wuhan to check the robustness of our model to the area size of study domain (Fig. S3). For each day, we converted the two-dimensional NO_2 column map over the domain to a one-dimensional line density along the wind direction (Text S3) (Beirle, 2011; Lorente et al., 2019). NO_x emissions and lifetimes can be estimated through the fitting of the NO_2 line density over the domain.

Lorente et al. (2019) presented a superposition model based on a column model (Jacob, 1999) to simulate NO_2 line density over Paris. They considered the build-up of NO_2 caused by spatially varying NO_x emissions from each cell and used the NO_2 line density value at the upwind end of the city to represent the background value, which they assumed to be constant over the city. This appears plausible if the background value would mostly represent free tropospheric NO_2 which has a longer lifetime than NO_2 in the oxidizing polluted boundary layer and varies smoothly according to models. Our method to simulate the NO_2 line density over the city is also based on the column model (Jacob, 1999), but differs from that of Lorente et al. (2019) in considering the background NO_2 value. Each cell along the wind direction is treated separately as a column model. NO_x emissions from the current cell contribute to the total line density through the build-up of NO_2 density within the cell and exponential decay of NO_2 downwind of the cell (Eq. (1)). It doesn't contribute to the upwind cells (Eq. (2)).

https://doi.org/10.5194/acp-2022-579
Preprint. Discussion started: 6 September 2022

Atmospheric Chemistry and Physics Discussions

$$N_i(x) = \frac{E_i}{k}\left(1 - e^{-kL/u}\right) \times e^{-k(x-x_i)/u} \times \frac{[NO_2]}{[NO_x]} \quad for\ x > x_i \ , \tag{1}$$

$$N_i(x) = 0 \qquad for\ x \le x_i \ , \tag{2}$$

where N_i represents the NO_2 line density (molec/cm) contributed from E_i in cell i, L is the length of each cell, i.e. 600000 cm; k is the loss rate (s^{-1}) of NO_x at 13:00 local time ($k = \frac{k'[OH]}{[NO_x]/[NO_2]}$); and u denotes the NO_2-density-weighted mean wind speed in unit of cm/s within planet boundary. We add up the contributions from each cell and the background value to model the overall NO_2 line density:

$$N(x) = \sum_{i=1}^{n} N_i(x) + b + \alpha x \ , \tag{3}$$

here, b represents the starting background value, equivalent to the mean NO_2 line density within the e-folding distance(Liu et al., 2016) upwind of x=0. α denotes the linear change of background value with distance along wind, and represents the chemical decay of background NO_2 flowing into the polluted boundary layer over the city.

We fit the terms that drive $N(x)$ (i.e. E_i, k and α) with the fixed L, u and $[NO_x]/[NO_2]$ from external data, via a least-squares minimization to the TROPOMI observed line density $N_{TROPOMI}(x)$. For each day, we run the model 20 times randomly choosing OH concentration within the ±20% interval of GEOS-Chem simulated OH concentration. The mean value from the 5 sets of parameters E_i, k and α that best explain the observations over the city is the answer we are seeking for. The parameter that describes the decay of upwind NO_2 over the city, the α value, is determined by the difference of NO_2 line density between the end and start point of the study domain, $\alpha = \frac{(N_{31} - N_1)}{30L}$, and we allow it to change between $\pm\alpha$in the fitting procedure. For the 50 days on average, the α value is $(-0.006 \pm 0.008) \times 10^{-22} molec/cm^2$. The α value being negative reflects the decay of upwind NO_2 pollution along the wind.

The assumption of a linearly decreasing NO_2 background is relevant under conditions when the city is in a polluted background. It accounts for decay of upwind NO_2 pollution arriving at the city when transported over and downwind of the city. In reality, upwind NO_2 pollution mixes in with the freshly emitted NO_x and is then subject to chemical decay (with non-linearities due to turbulent mixing and spatial heterogeneity in emissions). We acknowledge that our linear decrease of background NO_2 pollution is a severe simplification, but as shown in Fig. 1, compared to fitting results with a constant background value, we obtain a better correlation (up to 25%) between fitted and observed NO_2 line densities when fitting with a linearly changing background value.

https://doi.org/10.5194/acp-2022-579
Preprint. Discussion started: 6 September 2022

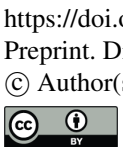

Atmospheric Chemistry and Physics Discussions

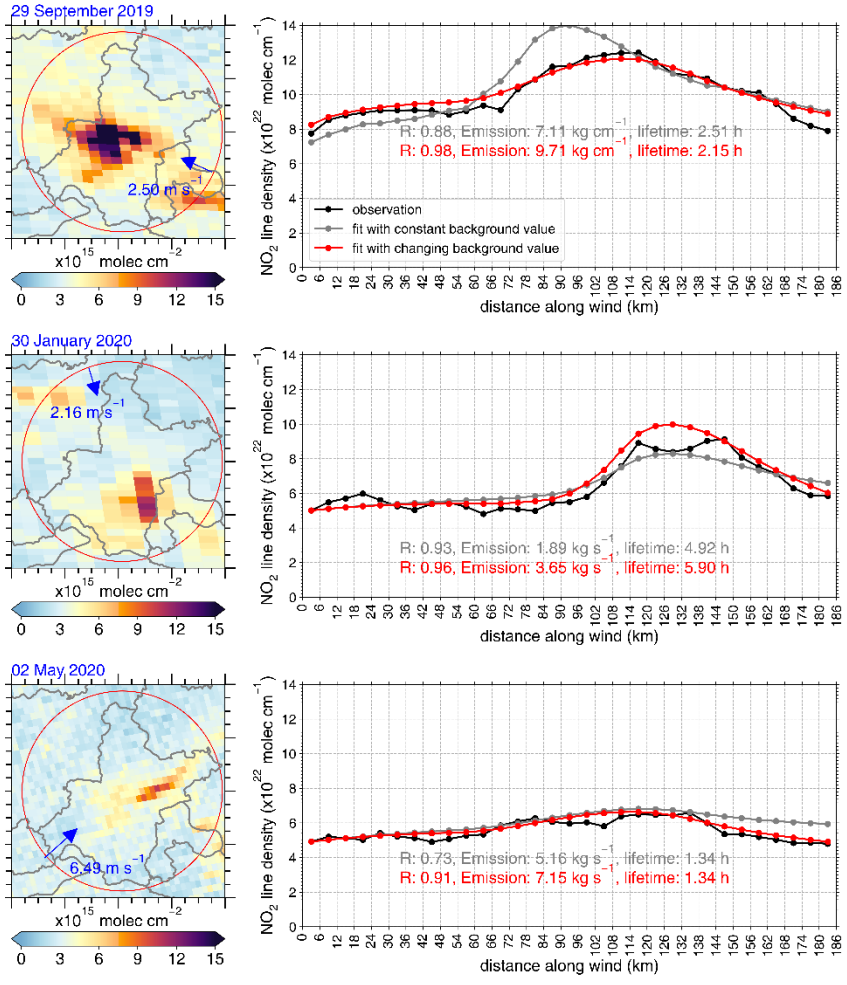

Figure 1: Tropospheric NO_2 columns over Wuhan on 29 September 2019, 30 January 2020 and 2 May 2020 (left, from top to bottom), the red circle inside each map defines the study domain. The corresponding NO_2 line densities along wind within the study domain are given in the right panel.

2.5 CO_2 emission estimation

City-scale CO_2 emissions are estimated through Eq. (4):

$$E_{CO_2} = E_{NO_x} \times Ratio_{CO_2-to-NO_x}, \quad (4)$$

The anthropogenic CO_2-to-NO_x emission ratio is provided by the ABACAS inventory, and amounts to ~591 gCO_2/gNO_x emitted from our study domain for the year 2019. In 2020, emissions from the transport sector have substantially decreased due to the lockdown measurements(Huang et al., 2021; Zheng et al., 2020c). The stronger decrease in transport NO_x emissions relative to decreases from other sectors are predicted to have led to an increase in the CO_2-to-NO_x emission ratio,

https://doi.org/10.5194/acp-2022-579
Preprint. Discussion started: 6 September 2022


Atmospheric Chemistry and Physics Discussions

for this ratio is lowest in the transport sector (Zheng et al., 2020c). The monthly CO_2-to-NO_x emission ratio for Wuhan were calculated based on recent reports on sectoral NO_x emission in 2020 from Hubei Province (Zheng et al., 2021a). We then further calculated daily CO_2-to-NO_x emission ratio based on the monthly, daily and diurnal variation of CO_2 and NO_x emissions (Fig. S5). The final daily CO_2-to-NO_x emission ratio for the study period displayed in Table S1 indeed shows increases in the CO_2-to-NO_x emission ratio of up to 20 % during the lockdown period in 2020.

2.6 uncertainty in NO_x and CO_2 emission estimation

Uncertainties in quantifying NO_x and CO_2 emissions contain the systematic error in the TROPOMI NO_2 retrieval, bias in the assumed a priori OH concentration, NO_x/NO_2 ratio, CO_2-to-NO_x emission ratio, uncertainties in wind fields and the area of study domain. The NO_2 column dataset S5P-PAL corrected the low bias in TROPOMI (v1.x) tropospheric NO_2 column over Eastern China by 15–100 % (Van Geffen et al., 2022). The CTMs have difficulty in simulating accurate OH concentration, but for > 90 % of the days, our fitted OH concentrations fall in ±20 % range around GEOS-Chem simulation, so the uncertainty in OH concentration is likely on the order of ±20 %. The difference between model simulated and observed NO_x/NO_2 ratio is less than 10 %, so we give an uncertainty in NO_x/NO_2 ratio of ±10 %. Uncertainty in CO_2-to-NO_x emission ratio comes from the errors in sectoral NO_x and CO_2 emissions, and we calculated that the uncertainty in CO_2-to-NO_x emission ratio is ±30 %. We have narrowed down our study domain to check the sensitivity of our method to the area of study domain (see Fig. S4). The results demonstrate that when the study domain is narrowed down to 84 km diameter, the change in fitted NO_x lifetime and NO_x emission is less than ±15%. We use the NO_2-column-weighted mean instead of the arithmetic mean value to get the boundary layer mean wind speed to minimize the error in wind field, but there may remain ±20 % uncertainty in the ERA5 reanalysis data. Considering that all these parameters are independent from each other, we use the root mean square sum of the contributions to represent the overall uncertainty estimation, which we quantify for NO_x lifetime and emission on a single day at ~37 %, and for CO_2 emission at ~48 %.

3 Results and discussion

3.1 NO_x Lifetimes and emissions

We display the calculated NO_x lifetime and NO_x emission for each clear-sky day during the study period in Table S1. Fitted planetary boundary layer mean OH concentration over the region for each day is presented in Fig. 2. For 90 % of the days, our model fitted OH concentrations which fall into the intervals of 0.8~1.2× the GEOS-Chem model values. There are only 5 days on which we had to impose a change in OH concentrations of more than 30 % relative to the GEOS-Chem simulation to obtain realistic fitting results.

.

https://doi.org/10.5194/acp-2022-579
Preprint. Discussion started: 6 September 2022

Atmospheric Chemistry and Physics Discussions

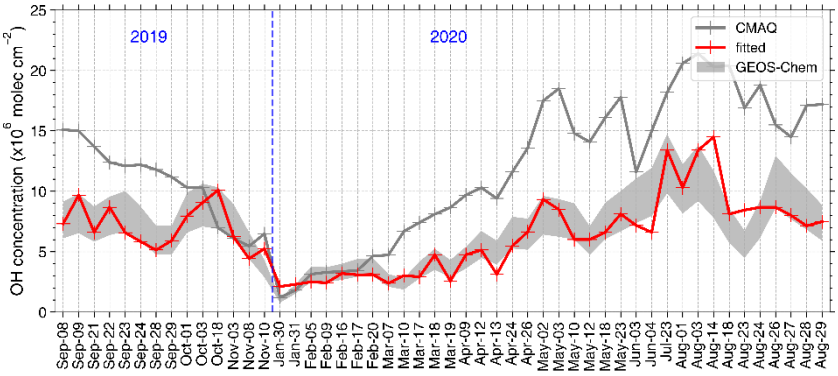

Figure 2: Boundary layer mean OH concentration over our study domain. The gray shade represents 0.8–1.2 times GEOS-Chem simulated OH concentration.

We estimate that seasonal mean noontime NO_x lifetime over Wuhan and adjacent region is 4.8±0.8 h for winter, 2.8±1.3 h for spring, 1.4±0.3 h for summer and 1.9±0.5 h for autumn. The results are lower than those calculated from GEOS-Chem simulation by Shah et al. (2020), with ~6 h in summer and >20 h in winter. This is because they calculated the 24-hour mean NO_x lifetime and the loss rate of NO_x is much higher around noon. NO_x lifetime for Wuhan is also shorter than for Paris (Lorente et al., 2019), especially during winter, reflecting the higher radiation levels and temperature in Wuhan than in Paris. It should be noted that Liu et al. (2016) fitted a NO_x lifetime of 2.6 h for Wuhan in warm season (May to September) for 2005–2013 mean, and our result for 2019-2020 is 1.7±0.4 h. One reason is that they calculated NO_x lifetimes based on a long-term mean NO_2 distribution, and the coarser resolution of OMI data, both of which lead to spatial smoothing of NO_2 gradients and thus longer apparent NO_x lifetimes (Qu, 2020). Another explanation is the increasing ozone concentrations in China in recent years (Li et al., 2020) which promote OH formation and thereby NO_x loss reactions which shorten NO_x lifetimes (Zara et al., 2021).

https://doi.org/10.5194/acp-2022-579
Preprint. Discussion started: 6 September 2022

Atmospheric Chemistry and Physics Discussions

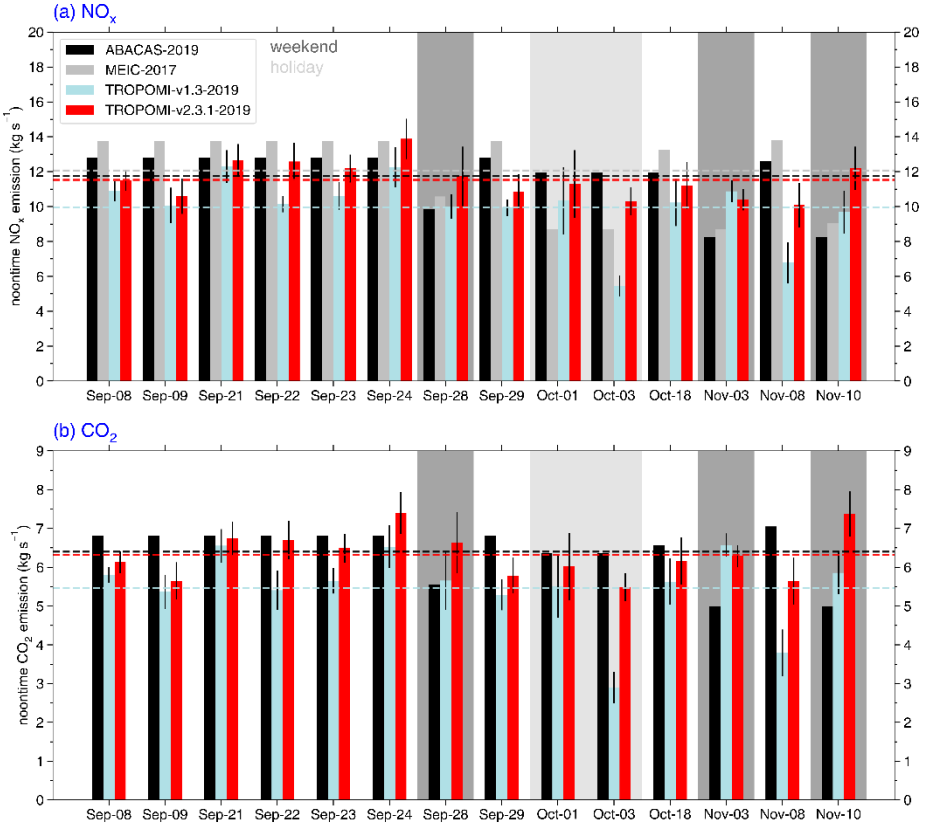

Figure 3: Daily noontime (a) NO_x and (b) CO_2 emission in Wuhan estimated from TROPOMI (red and blue bars, the error bars represent the standard deviation of the five best estimates for each day) and the bottom-up emission inventories ABACAS (black bars) for the year 2019 and MEIC (silver bars) for the year 2017. The dark and light grey shades represents weekends and holidays, respectively. Mean levels of each dataset are given as dashed lines with corresponding colors.

The calculated noontime (13:00 local time) NO_x emissions from Wuhan for 14 days (including 9 weekdays, 3 weekends and 2 holidays) between September and November 2019 are compared with those from the ABACAS (2019) and MEIC (2017) inventories. Overall, as presented in Fig. 3a, the rescaled TROPOMI-v1.3 estimated noontime NO_x emissions are 13.6% lower than those from TROPOMI-v2.3.1. Compared to the bottom-up emission inventories, TROPOMI-v1.3-2019 NO_x emissions are 15.1 % and 17.5 % lower than ABACAS-2019 and MEIC-2017, respectively. On the other hand, TROPOMI-v2.3.1-2019 NO_x emissions are comparable to those from ABACAS-2019 (< 3 % difference), and ~5 % lower than MEIC-2017. That NO_x emissions estimated from TROPOMI-v2.3.1 in 2019 are lower than MEIC-2017 likely reflects the fact that NO_x emissions have decreased in 2019 relative to 2017 in response to Chinese emission controls. According to Wuhan Bureau of Statistics, NO_x emissions have decreased 6.2 % between 2017 and 2019 (Statistics, 2019; Bauwens et al., 2020), close to the difference between TROPOMI-v2.3.1-2019 and MEIC-2017. TROPOMI-v2.3.1 NO_2 data generates more reliable NO_x emissions from Wuhan in 2019 than the v1.3 data, even when the latter is scaled up by a factor of 1.6.

https://doi.org/10.5194/acp-2022-579
Preprint. Discussion started: 6 September 2022


Atmospheric Chemistry and Physics Discussions

Different to the bottom-up inventories, our daily TROPOMI NO_x emissions do not indicate the existence of a so-called 'weekend reduction effect', but do point out a distinct 'holiday reduction effect' in Wuhan NO_x emissions. The bottom-up inventories suggest that weekend NO_x emissions are 30 % reduced relative to weekdays. The TROPOMI estimation shows reductions in weekend NO_x emission of < 3 %, while on the two days (1 and 3 October) of the National Holiday, NO_x emissions are 8% lower than the workday mean. Surface NO_2 and O_3 observations from Beijing do not show a weekend effect (Zhao et al., 2019; Hua et al., 2021) either. Our TROPOMI NO_x emissions show a similar spatial pattern as in ABACAS and MEIC (Fig. S1), with the highest emissions located in the city center of Wuhan. However, TROPOMI fitted a more smeared-out NO_x emission pattern than ABACAS, due to the strong dependence of the bottom-up spatial distribution on population density, the difference in spatial resolution, and the decrease in NO_x emission between 2017 and 2020 mainly occurring in the high-emission region.

3.2 CO_2 emissions and XCO_2 enhancements

We estimate noontime CO_2 emissions from Wuhan between September and November 2019 to be 6.32±0.60 s^{-1}, comparable to ABACAS-2019, of 6.40±0.70 t s^{-1} (Fig. 3b). Based on the estimated daily CO_2 emissions, we further use the superposition column model to estimate daily XCO_2 enhancements, and validate them by OCO-2 observations. We successfully obtained two days between May 2018 (start time of TROPOMI-v2.3.1 NO_2 product) and December 2021 with simultaneous (both overpass at around 13:00 local time), co-located TROPOMI NO_2 and OCO-2 CO_2 observations over Wuhan: 15 September 2018 and 13 April 2020. We inferred total CO_2 emissions from Wuhan based on our TROPOMI-based NO_x emissions and the ABACAS-predicted CO_2-to-NO_x emission ratios on 15 September 2018 and 13 April 2020 to be 7.92±0.93 t s^{-1} and 4.44±0.50 t s^{-1} (the errors represent the standard deviation of the 5 best estimations for each day), respectively. We then scaled down the ABACAS 1×1 km^2 gridded CO_2 emissions to match 7.92 t s^{-1} and 4.44 t s^{-1}, and then predict the XCO_2 enhancements using the top-down CO_2 emissions in combination with the superposition column model. It should be noted that to compare with the sparse distributed OCO-2 observations, we apply the superposition model on the CO_2 line density with 1km wide, while it is 186km wide for NO_2. Since that the column model doesn't take the dispersion of NO_2 or CO_2 into account, all dispersion will then be encapsulated within the domain when a line density covers cross-section as wide as 186 km. However, when the line density is only 1 km wide, the dispersion will move CO_2 out of this line, and we will discuss its influence on CO_2 enhancement estimation in the further below.

Neglecting chemical production and loss of CO_2 in the atmosphere, the superposition column model of CO_2 (Eq. 5) is simpler than that of NO_x:

$$N_{CO_2} = \frac{E_{CO_2}}{uL}, \quad (5)$$

https://doi.org/10.5194/acp-2022-579
Preprint. Discussion started: 6 September 2022

Atmospheric Chemistry and Physics Discussions

Here N_{CO_2} is CO_2 density in unit of g m^{-2}, E_{CO_2} denotes our top-down CO_2 emission (g s^{-1}), and u and L are the wind speed (m/s) and length of grid cell (6000 m). Then N_{CO_2}(g m^{-2}) is converted to the column mixing ratio XCO_2 (ppm) to compare with the OCO-2 observation (Zheng et al., 2020a):

$$XCO_2 = N_{CO_2} \times \frac{M_{air}}{M_{CO_2}} \times \frac{g}{p - wg} \times 10^3 \,, \tag{6}$$

in which M_{air} and M_{CO_2} are air and CO_2 molar mass of air and CO_2 (g mol^{-1}), g is the gravitational acceleration (9.8 m/s^2), p (Pa) and w (kg m^{-2}) are surface pressure and total column water vapor, respectively.

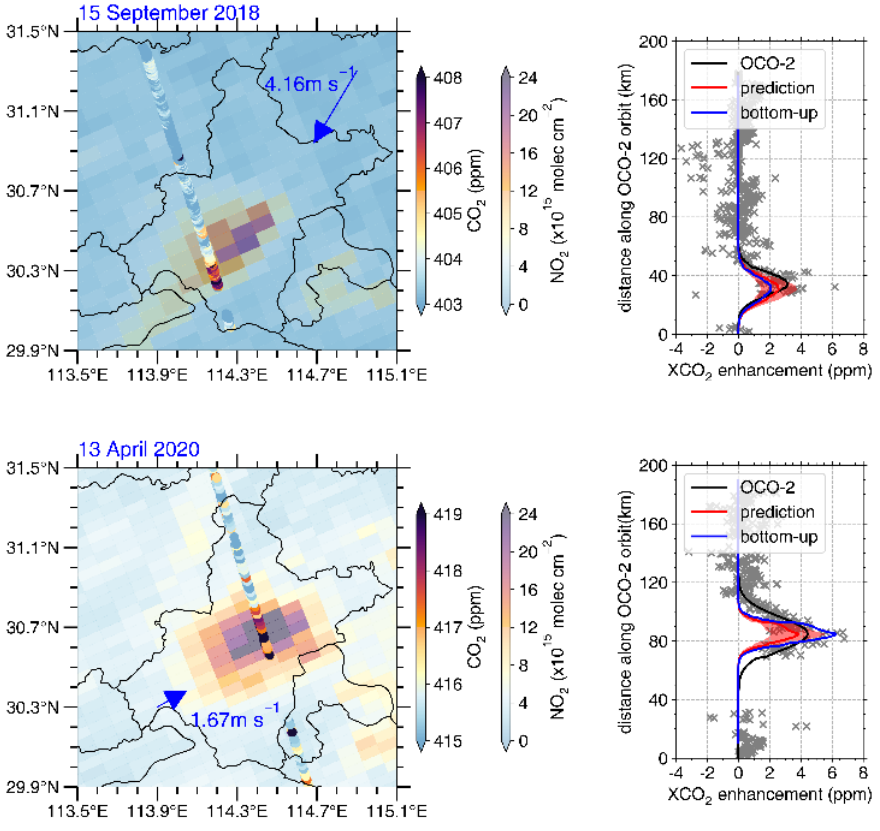

Figure 4: Simultaneous, co-located TROPOMI NO_2 and OCO-2 CO_2 observations over Wuhan (left panel) on 15 September 2018 (top) and 13 April 2020 (bottom), wind speed and direction on each day are shown. The dry air mole fraction of CO_2 (XCO_2) enhancements along the OCO-2 orbit are given for corresponding day (right panel). The gray xs and black lines represent the OCO-2 observation. The blue lines denote XCO_2 enhancement estimated with bottom-up emissions, and the red lines (shading represents the uncertainty interval) with CO_2 emission predicted in this study.

We calculate the XCO_2 enhancement due our top-down CO_2 emissions on 15 September 2018 and 13 April 2020 and compare these with the enhancements observed by OCO-2. As shown in the right panels of Fig. 4, the superposition model captures the spatial pattern of observed XCO_2 along the OCO-2 orbit on both days. The predicted amplitudes of the XCO_2

https://doi.org/10.5194/acp-2022-579
Preprint. Discussion started: 6 September 2022


Atmospheric Chemistry and Physics Discussions

enhancements are also comparable to those in the OCO-2 observation with small bias (less than 5 % for both days). As comparison, we also use the 2019 bottom-up CO_2 emissions to predict the XCO_2 enhancement on the two days (blue lines in Fig. 4 right panel). XCO_2 enhancements predicted by bottom-up CO_2 emissions deviate more from the OCO-2 observed enhancements than those predicted by our top-down CO_2 emissions. On 13 April 2020 in particular, the bottom-up enhancement differs by +41% while the top-down differs by only within ±5 % compared to the observed XCO_2 enhancement. At the beginning of Wuhan's reopening, CO_2 emission from the city (our top-down estimation) is expected to be far lower than the pre-lockdown level (bottom-up estimation).

We see that the estimated XCO_2 enhancement on 13 April 2020, both from the bottom-up and top-down emissions, are much 'narrower' compared to the OCO-2 observation. On this day, the OCO-2 orbit passes over the city center and the dispersion plays an important role, which is neglected in the column model. In contrast, on 15 September 2018, the OCO-2 orbit passes downwind of the city center, and the width of the estimated and observed XCO_2 enhancements are more comparable. For comparison, we also conducted a Gaussian plume model to estimate XCO_2 enhancement (Text S4 and Fig. S6). On 13 April 2020, the result from Gaussian model agrees better with the OCO-2 observation, and on 15 September 2018, results from the two models (Gaussian model and the superposition column model) are close to each other and match well with the observation.

We also display XCO_2 enhancement line densities along wind direction with uncertainty on both days (Fig. 5). The line density shows a substantial increase of XCO_2 along the wind direction over the region with strong CO_2 emissions (Fig.5a, b, the inset maps). Where lines cross the OCO-2 orbit, the observed XCO_2 (as boxplots in Fig. 5a, b) are shown and their values agree with the predicted XCO_2 lines within ±0.3 ppm. It is remarkable that the XCO_2 enhancement is lower on 15 September 2018 than on 13 April 2020, despite CO_2 emissions on 15 September 2018 being nearly 65 % higher than those on 13 April 2020. The main reason for this is the lower wind speed on 13 April 2020, which accumulates pollutants over the city, and the fact that OCO-2 ground-track passed over the city center of Wuhan on this day. On 15 September, higher wind speeds and the OCO-2 track being situated over the outskirts of the city imply that a lower enhancement of CO_2 is observed.

https://doi.org/10.5194/acp-2022-579
Preprint. Discussion started: 6 September 2022

Atmospheric Chemistry and Physics Discussions

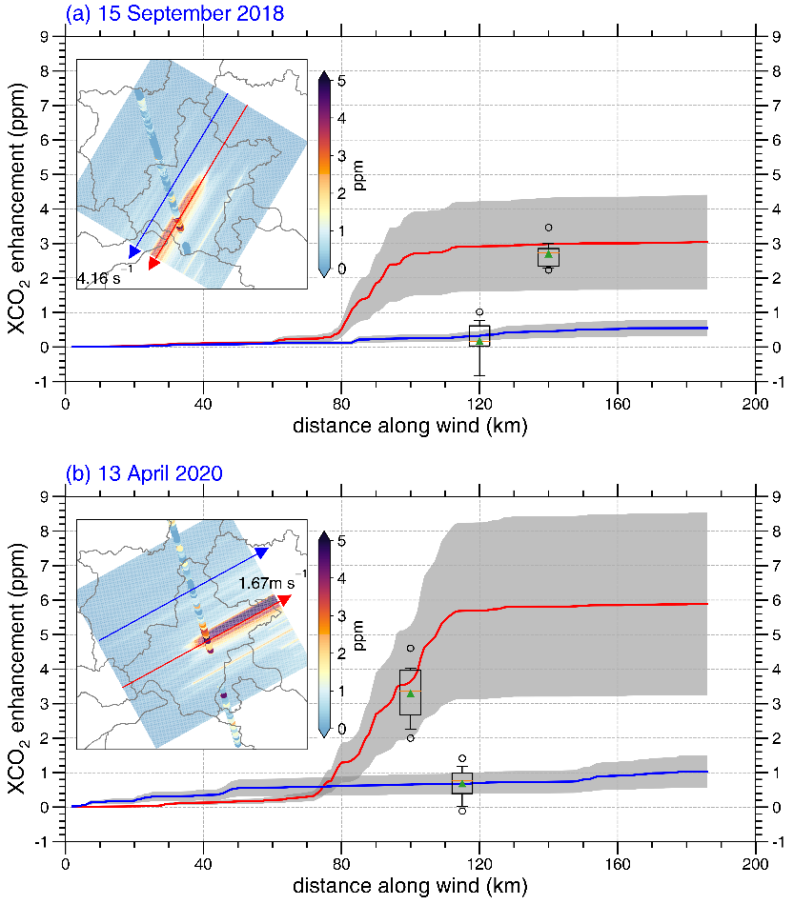

290 **Figure 5: Two presentative predicted XCO_2 enhancement lines (red and blue) on (a) 15 September 2018 and (b) 13 April 2020. When the XCO_2 enhancement line pass through the OCO-2 orbit, the observed XCO_2 enhancements are shown with boxplots, the mean values are shown as green triangles, the outliers beyond the 5–95 % interval are shown as circles. The predicted XCO_2 enhancement line density maps overlayed with OCO-2 observed XCO_2 enhancement on each day are shown inside, with the position of the presentative lines and the wind direction.**

295 We use an 'indirect' method to estimate daily city anthropogenic CO_2 emissions and XCO_2 enhancements, which may introduce uncertainties from the NO_x emission estimation, the assumption of CO_2-to-NO_x emission ratio, and the model to estimate XCO_2 enhancements. Despite all these uncertainties, we still generate daily Wuhan CO_2 emissions and XCO_2 enhancements that agree well with bottom-up inventory and OCO-2 observation, respectively.

3.3 Variation of NO_x and CO_2 emissions in Wuhan from September 2019 to August 2020

300 Figure 6 displays the day-to-day variation of NO_x and CO_2 emissions in Wuhan between September 2019 and August 2020. Before the pandemic of COVID-19, NO_x emissions stay at a stable level of 11.53±1.08 kg s^{-1}, and CO_2 at 6.32±0.66 t s^{-1}, as

https://doi.org/10.5194/acp-2022-579
Preprint. Discussion started: 6 September 2022

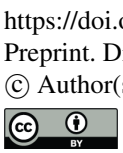

Atmospheric Chemistry and Physics Discussions

indicated by the dashed red lines. From January 2020 onwards, strict lockdown measurements were implemented to combat the COVID-19 pandemic, which led to lower industry production and less traffic on the road, and a sharp drop in NO_x and CO_2 emissions (Ding et al., 2020; Zhang et al., 2020; Zheng et al., 2021b; Zhang et al., 2021; Feng et al., 2020). Our method closely captures the timing and magnitude of these well-known sharp reductions in the emissions.

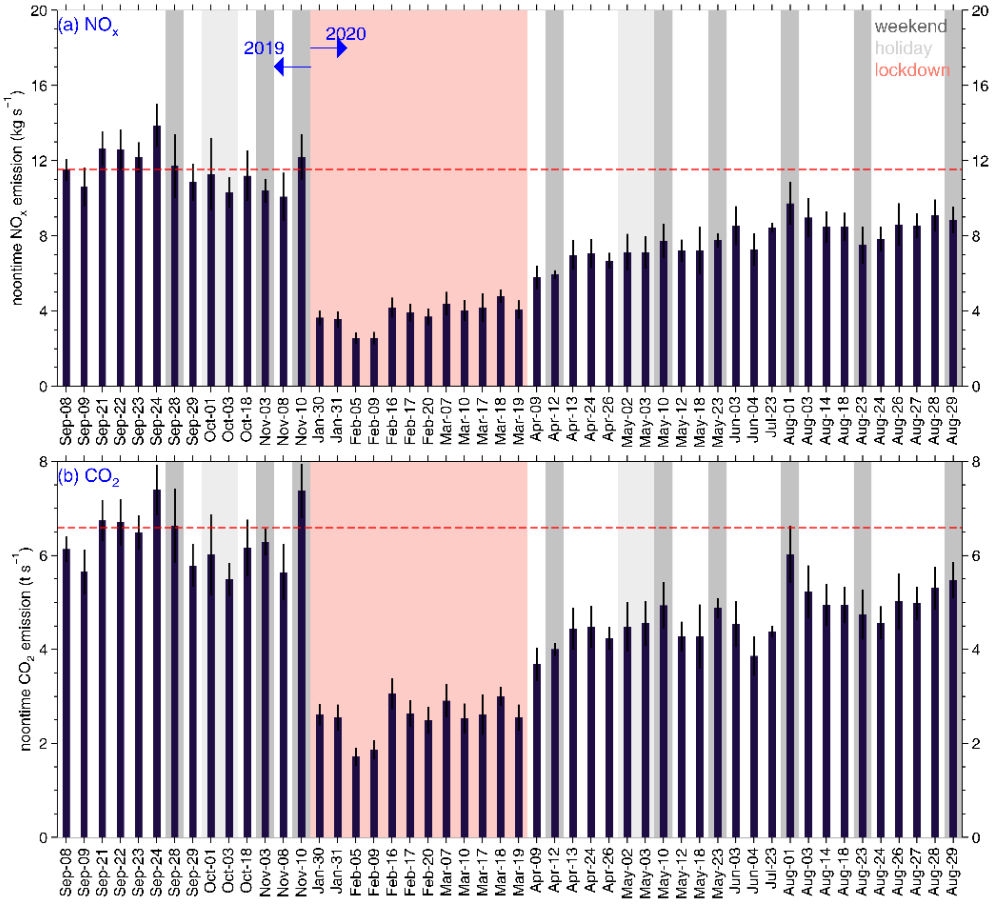

Figure 6: 50 days (a) NO_x and (b) CO_2 emissions in Wuhan estimated from TROPOMI from September 1 2019 to August 31 2020. The error bars denote the standard deviation of the five best estimates for each day, and the weekends, holidays and lockdown period are shaded with dark grey, light grey and red colors, respectively. The mean pre-lockdown emission levels are given as red dashed lines.

Wuhan NO_x emissions on 30 January 2020 are 3.65±0.36 kg s^{-1}, nearly 70 % lower than pre-lockdown levels, and decreased further and came to the lowest level in early February 2020, in accordance with Feng et al. (2020) who estimated similar reductions based on surface NO_2 observations. 5 February is the day with our lowest NO_x emission from Wuhan of 2.55±0.31 kg s^{-1}, only ~22 % of the normal level. CO_2 emissions have a similar temporal pattern as NO_x emissions, but the reduction relative to pre-lockdown level is smaller. The lowest CO_2 emission is at ~27 % of the pre-lockdown level (also on

https://doi.org/10.5194/acp-2022-579
Preprint. Discussion started: 6 September 2022


Atmospheric Chemistry and Physics Discussions

5 February 2020), and the mean emission rate during the lockdown period (23 January to 8 April 2020) is 60 % lower than pre-lockdown level, while it is 67 % for NO_x. That CO_2 emission reductions are more modest than NO_x reductions reflects the fact that the transportation sector had the strongest reductions during the lockdown, but since this sector also has the lowest CO_2-to-NO_x ratios, the relative reduction in CO_2 remains somewhat smaller than in NO_x emissions. This finding is similar to that from Zheng et al. (2020b), who estimated the NO_x and CO_2 emission variations for whole China.

From early February 2020 onwards, emissions increased slowly throughout the lockdown period. Wuhan NO_x emission intensity in February 2020 was no more than 4.20 kg s^{-1}, some 60 % below the pre-lockdown level. Feng et al. (2020) estimated 61 % lower NO_x emission from Wuhan in February 2020 than January based on surface NO_x observations. Zheng et al. (2021a) reported a ~50 % lower NO_x emission from Hubei in February 2020 than the annual mean level estimated from a bottom-up approach.

Although Wuhan reopened on 9 April, the NO_x and CO_2 emissions didn't see significant increases up until mid-May 2020. A perceptible increase in NO_x emission is seen during late May, climbing to > 7.50 kg s^{-1} (NO_x) and > 4.5 t s^{-1} (CO_2), and leveling off thereafter. In August 2020, Wuhan NO_x emissions were still some 25 % lower than the pre-lockdown level. Although bottom-up estimation by Zheng et al. (2021a) suggested that NO_x emissions from the Hubei province were similar in May–August 2020 as in 2019, surface and satellite observations over Wuhan show a 15–20 % lower NO_2 concentrations in May–August 2020 compared to 2019 (Fig. S7 and S8), consistent with our estimation of NO_x emission. Liu et al. (2020c) reported 4.8 % higher CO_2 emissions for the whole China in August 2020 compared to August 2019. For the city of Wuhan, however, we calculate here some 20 % lower CO_2 emissions in August 2020 compared to the pre-lockdown level. Wuhan experienced a much more strict and longer period lockdown than other regions of China, and therefore a slower rebound of NO_x and CO_2 emissions should be expected over Wuhan.

4 Conclusion

In this study, we introduced an improved superposition column model to estimate daily NO_x and CO_2 emissions from a Chinese megacity of Wuhan based on the latest released version 2.3.1 of TROPOMI NO_2 column data and OCO-2 XCO_2 observation. Our estimated daily NO_x and CO_2 emissions agree well with bottom-up emissions with small bias of < 3 %. Predicted XCO_2 enhancements based on our CO_2 emissions estimates prove to be in good agreement (within ±5 %) with OCO-2 observations over Wuhan. Compared to previous studies, our work shows that satellite measurements can provide detailed information on city-scale NO_x and CO_2 emissions at unprecedented spatial and temporal resolutions. We achieved the day-to-day variation of NO_x and CO_2 emissions from Wuhan between September 2019 and August 2020. We pointed out that the 'weekend reduction' is small, but that a 'holiday reduction' in Wuhan NO_x and CO_2 emissions can be clearly detected. We also captured the abrupt decrease in NO_x and CO_2 emissions as the lockdown for COVID began on 23 January 2020, and the slow rebound as Wuhan reopened on 9 April 2020. Daily updates of city-scale NO_x and CO_2 emissions provides policy makers with emission and policy control data on NO_x and CO_2 emission control in urban environment.

https://doi.org/10.5194/acp-2022-579
Preprint. Discussion started: 6 September 2022


Atmospheric Chemistry and Physics Discussions

In the future, following the launch of the Carbon Dioxide Monitoring mission (CO2M)(Sierk et al., 2021), our improved superposition column method may be explored further to constrain city scale CO_2 and NO_x emissions to assess the effectiveness of emission control measures. CO2M provides simultaneous and co-located CO_2 and NO_2 observations with a wider swath than OCO-2, providing better opportunities to verify and improve CO_2 and NO_x emissions from space.

.

Author contributions. Q.Z. and K.F.B designed the research; Q.Z. performed the data analysis, model development and result validation. B.Z. and H.Z. provide the ABACAS-EI NO_x and CO_2 emission inventories. H.E. provides the 2.3.1 version of TROPOMI tropospheric NO_2 product. C.C. provides MEIC NO_x emissions and perform the CMAQ simulations. X. Z. provided helpful discussions. Q.Z. and K.F.B. wrote the paper.

Competing interests. The authors declare no competing financial interest.

Acknowledgement. This work is funded by the National Natural Science Foundation of China (No.: 41805098) and the China Scholarship Council (202005330023). Improvements in TROPOMI NO_2 data have received support from the KNMI MSO NO_2NEXT project.

References

Bauwens, M., Compernolle, S., Stavrakou, T., Muller, J. F., van Gent, J., Eskes, H., Levelt, P. F., van der, A. R., Veefkind, J. P., Vlietinck, J., Yu, H., and Zehner, C.: Impact of coronavirus outbreak on NO_2 pollution assessed using TROPOMI and OMI observations, Geophys. Res. Lett., e2020GL087978, 10.1029/2020GL087978, 2020.

Beirle, S., Boersma, K. F., Platt, U., Lawrence, M. G., and Wagner, T.: Megacity emissions and lifetimes of nitrogen oxides probed from space, Science, 333, 1737-1739, 10.1126/science.1207824, 2011.

Beirle, S. B., K.F., Platt, U., Lawrence, M.G., Wagner, T.: Megacity Emissions and Lifetimes of Nitrogen Oxides Probed from Space, Science, 333, 2011.

Berezin, E. V., Konovalov, I. B., Ciais, P., Richter, A., Tao, S., Janssens-Maenhout, G., Beekmann, M., and Schulze, E. D.: Multiannual changes of CO_2 emissions in China: indirect estimates derived from satellite measurements of tropospheric NO_2 columns, Atmos. Chem. Phys., 13, 9415-9438, 10.5194/acp-13-9415-2013, 2013.

Ding, J., A, R. J., Eskes, H. J., Mijling, B., Stavrakou, T., Geffen, J. H. G. M., and Veefkind, J. P.: NO_x Emissions Reduction and Rebound in China Due to the COVID-19 Crisis, Geophys. Res. Lett., 47, 10.1029/2020gl089912, 2020.

Eskes, H., Van Geffen, J., Sneep, M., Veefkind, J. P., Niemeijer, S., and Zehner, C.: S5P Nitrogen Dioxide v02.03.01 intermediate reprocessing on the S5P-PAL system: Readme file, 2021.

Feng, S., Jiang, F., Wang, H., Wang, H., Ju, W., Shen, Y., Zheng, Y., Wu, Z., and Ding, A.: NO_x Emission Changes Over China During the COVID-19 Epidemic Inferred From Surface NO_2 Observations, Geophys. Res. Lett., 47, e2020GL090080, 10.1029/2020GL090080, 2020.

Griffin, D., McLinden, C. A., Boersma, F., Bourassa, A., Dammers, E., Degenstein, D., Eskes, H., Fehr, L., Fioletov, V., Hayden, K., Kharol, S. K., Li, S. M., Makar, P., Martin, R. V., Mihele, C., Mittermeier, R. L., Krotkov, N., Sneep, M., Lamsal, L. N., Ter Linden, M., van Geffen, J., Veefkind, P., Wolde, M., and Zhao, X.: High resolution mapping of nitrogen dioxide with TROPOMI: First results and validation over the Canadian oil sands, Geophys. Res. Lett., 46, 1049-1060, 10.1029/2018GL081095, 2019.

https://doi.org/10.5194/acp-2022-579
Preprint. Discussion started: 6 September 2022

Atmospheric Chemistry and Physics Discussions

Gunson M and Eldering, A.: OCO-2 Level 2 bias-corrected XCO_2 and other select fields from the full-physics retrieval aggregated as daily files, Retrospective processing V10r, Greenbelt, MD, USA, Goddard Earth Sciences Data and Information Services Center (GES DISC), last access: 31-05-2022, 10.5067/E4E140XDMPO2, 2020.

Hersbach, H., Bell, B., Berrisford, P., Hirahara, S., Horányi, A., Muñoz-Sabater, J., Nicolas, J., Peubey, C., Radu, R., Schepers, D., Simmons, A., Soci, C., Abdalla, S., Abellan, X., Balsamo, G., Bechtold, P., Biavati, G., Bidlot, J., Bonavita, M., Chiara, G., Dahlgren, P., Dee, D., Diamantakis, M., Dragani, R., Flemming, J., Forbes, R., Fuentes, M., Geer, A., Haimberger, L., Healy, S., Hogan, R. J., Hólm, E., Janisková, M., Keeley, S., Laloyaux, P., Lopez, P., Lupu, C., Radnoti, G., Rosnay, P., Rozum, I., Vamborg, F., Villaume, S., and Thépaut, J. N.: The ERA5 global reanalysis, Q J R Meteorol Soc., 146, 1999-2049, 10.1002/qj.3803, 2020.

Hua, J., Zhang, Y., de Foy, B., Mei, X., Shang, J., and Feng, C.: Competing $PM_{2.5}$ and NO_2 holiday effects in the Beijing area vary locally due to differences in residential coal burning and traffic patterns, Sci. Total. Environ., 750, 141575, 10.1016/j.scitotenv.2020.141575, 2021.

Huang, X., Ding, A., Gao, J., Zheng, B., Zhou, D., Qi, X., Tang, R., Wang, J., Ren, C., Nie, W., Chi, X., Xu, Z., Chen, L., Li, Y., Che, F., Pang, N., Wang, H., Tong, D., Qin, W., Cheng, W., Liu, W., Fu, Q., Liu, B., Chai, F., Davis, S. J., Zhang, Q., and He, K.: Enhanced secondary pollution offset reduction of primary emissions during COVID-19 lockdown in China, Natl Sci Rev., 8, nwaa137, 10.1093/nsr/nwaa137, 2021.

Jacob, D.: Introduction to Atmospheric Chemistry, Princeton Univ. Press, 1999.

Lamsal, L. N., Martin, R. V., Padmanabhan, A., van Donkelaar, A., Zhang, Q., Sioris, C. E., Chance, K., Kurosu, T. P., and Newchurch, M. J.: Application of satellite observations for timely updates to global anthropogenic NO_x emission inventories, Geophys. Res. Lett., 38, n/a, 10.1029/2010gl046476, 2011.

Lamsal, L. N., Martin, R. V., van Donkelaar, A., Celarier, E. A., Bucsela, E. J., Boersma, K. F., Dirksen, R., Luo, C., and Wang, Y.: Indirect validation of tropospheric nitrogen dioxide retrieved from the OMI satellite instrument: Insight into the seasonal variation of nitrogen oxides at northern midlatitudes, J. Geophys. Res., 115, 10.1029/2009jd013351, 2010.

Li, K., Jacob, D. J., Shen, L., Lu, X., De Smedt, I., and Liao, H.: Increases in surface ozone pollution in China from 2013 to 2019: anthropogenic and meteorological influences, Atmos. Chem. Phys., 20, 11423-11433, 10.5194/acp-20-11423-2020, 2020.

Li, M., Zhang, Q., Kurokawa, J.-i., Woo, J.-H., He, K., Lu, Z., Ohara, T., Song, Y., Streets, D. G., Carmichael, G. R., Cheng, Y., Hong, C., Huo, H., Jiang, X., Kang, S., Liu, F., Su, H., and Zheng, B.: MIX: a mosaic Asian anthropogenic emission inventory under the international collaboration framework of the MICS-Asia and HTAP, Atmos. Chem. Phys., 17, 935-963, 10.5194/acp-17-935-2017, 2017.

Liu, F., Beirle, S., Zhang, Q., Dörner, S., He, K., and Wagner, T.: NO_x lifetimes and emissions of cities and power plants in polluted background estimated by satellite observations, Atmos. Chem. Phys., 16, 5283-5298, 10.5194/acp-16-5283-2016, 2016.

Liu, F., Duncan, B. N., Krotkov, N. A., Lamsal, L. N., Beirle, S., Griffin, D., McLinden, C. A., Goldberg, D. L., and Lu, Z.: A methodology to constrain carbon dioxide emissions from coal-fired power plants using satellite observations of co-emitted nitrogen dioxide, Atmos. Chem. Phys., 20, 99-116, 10.5194/acp-20-99-2020, 2020a.

Liu, M., Lin, J., Kong, H., Boersma, K. F., Eskes, H., Kanaya, Y., He, Q., Tian, X., Qin, K., Xie, P., Spurr, R., Ni, R., Yan, Y., Weng, H., and Wang, J.: A new TROPOMI product for tropospheric NO_x columns over East Asia with explicit aerosol corrections, Atmos. Meas. Tech., 13, 4247-4259, 10.5194/amt-13-4247-2020, 2020b.

Liu, Z., Ciais, P., Deng, Z., Davis, S. J., Zheng, B., Wang, Y., Cui, D., Zhu, B., Dou, X., Ke, P., Sun, T., Guo, R., Zhong, H., Boucher, O., Breon, F. M., Lu, C., Guo, R., Xue, J., Boucher, E., Tanaka, K., and Chevallier, F.: Carbon Monitor, a near-real-time daily dataset of global CO_2 emission from fossil fuel and cement production, Sci. Data, 7, 392, 10.1038/s41597-020-00708-7, 2020c.

Lorente, A., Boersma, K. F., Eskes, H. J., Veefkind, J. P., van Geffen, J., de Zeeuw, M. B., Denier van der Gon, H. A. C., Beirle, S., and Krol, M. C.: Quantification of nitrogen oxides emissions from build-up of pollution over Paris with TROPOMI, Sci. Rep., 9, 20033, 10.1038/s41598-019-56428-5, 2019.

ODell, C., Eldering, A., Gunson , M., Crisp, D., Fisher, B., Kiel, M., Kuai, L., Laughner, J., Merrelli, A., Nelson, R., Osterman, G., Payne, V., Rosenberg, R., Taylor, T., Wennberg, P., Kulawik, S., Lindqvist, H., Miller, S., and Nassar, R.: Improvements in XCO_2 accuracy from OCO-2 with the latest ACOS v10 product, EGU General Assembly 2021, online, 19–30 Apr 2021, EGU21-10484, 2021.

Qu, H.: Summertime ozone pollution over China: observations and simulations, Dissertation for the degree of Doctor of Philosophy, School of Earth and Atmospheric Science, Georfia Institute of Technology, 2020.

Reuter, M., Buchwitz, M., Schneising, O., Krautwurst, S., O'Dell, C. W., Richter, A., Bovensmann, H., and Burrows, J. P.: Towards monitoring localized CO_2 emissions from space: co-located regional CO_2 and NO_2 enhancements observed by the OCO-2 and S5P satellites, Atmos. Chem. Phys., 19, 9371-9383, 10.5194/acp-19-9371-2019, 2019.

Reuter, M., Buchwitz, M., Hilboll, A., Richter, A., Schneising, O., Hilker, M., Heymann, J., Bovensmann, H., and Burrows, J. P.: Decreasing emissions of NO_x relative to CO_2 in East Asia inferred from satellite observations, Nature Geosci., 7, 792-795, 10.1038/ngeo2257, 2014.

Riess, T. C. V. W., Boersma, K. F., van Vliet, J., Peters, W., Sneep, M., Eskes, H., and van Geffen, J.: Improved monitoring of shipping NO_2 with TROPOMI: decreasing NO_x emissions in European seas during the COVID-19 pandemic, Atmos. Meas. Tech., 15, 1415-1438, 10.5194/amt-15-1415-2022, 2022.

https://doi.org/10.5194/acp-2022-579
Preprint. Discussion started: 6 September 2022

Atmospheric Chemistry and Physics Discussions

Shah, V., Jacob, D. J., Li, K., Silvern, R. F., Zhai, S., Liu, M., Lin, J., and Zhang, Q.: Effect of changing NO_x lifetime on the seasonality and long-term trends of satellite-observed tropospheric NO_2 columns over China, Atmos. Chem. and Phys., 20, 1483-1495, 10.5194/acp-20-1483-2020, 2020.

Sierk, B., Fernandez, V., Bézy, J. L., Meijer, Y., Durand, Y., Bazalgette Courrèges-Lacoste, G., Pachot, C., Löscher, A., Nett, H., Minoglou, K., Boucher, L., Windpassinger, R., Pasquet, A., Serre, D., te Hennepe, F., Sodnik, Z., Cugny, B., and Karafolas, N.: The Copernicus CO2M mission for monitoring anthropogenic carbon dioxide emissions from space, International Conference on Space Optics — ICSO 2020, 10.1117/12.2599613, 2021.

Statistics, W. B. o.: Statistical Bulletin on domestic economic and social development of Wuhan (2018), http://tjj.wuhan.gov.cn/tjfw/tjgb/202001/t20200115_841065.shtml (in Chinese, last access: 2022-05-19), 2019.

van Geffen, J., Boersma, K. F., Eskes, H., Sneep, M., ter Linden, M., Zara, M., and Veefkind, J. P.: S5P TROPOMI NO_2 slant column retrieval: method, stability, uncertainties and comparisons with OMI, Atmos. Meas. Tech., 13, 1315-1335, 10.5194/amt-13-1315-2020, 2020.

van Geffen, J., Eskes, H., Compernolle, S., Pinardi, G., Verhoelst, T., Lambert, J.-C., Sneep, M., ter Linden, M., Ludewig, A., Boersma, K. F., and Veefkind, J. P.: Sentinel-5P TROPOMI NO_2 retrieval: impact of version v2.2 improvements and comparisons with OMI and ground-based data, Atmos. Meas. Tech., 15, 2037-2060, 10.5194/amt-15-2037-2022, 2022.

Visser, A. J., Boersma, K. F., Ganzeveld, L. N., and Krol, M. C.: European NO_x emissions in WRF-Chem derived from OMI: impacts on summertime surface ozone, Atmos. Chem. Phys., 19, 11821-11841, 10.5194/acp-19-11821-2019, 2019.

Wang, C., Wang, T., Wang, P., and Rakitin, V.: Comparison and Validation of TROPOMI and OMI NO2 Observations over China, Atmosphere, 11, 10.3390/atmos11060636, 2020.

Zara, M., Boersma, K. F., Eskes, H., Denier van der Gon, H., Vilà-Guerau de Arellano, J., Krol, M., van der Swaluw, E., Schuch, W., and Velders, G. J. M.: Reductions in nitrogen oxides over the Netherlands between 2005 and 2018 observed from space and on the ground: Decreasing emissions and increasing O_3 indicate changing NO_x chemistry, Atmos. Environ.: X, 9, 10.1016/j.aeaoa.2021.100104, 2021.

Zhang, Q., Pan, Y., He, Y., Walters, W. W., Ni, Q., Liu, X., Xu, G., Shao, J., and Jiang, C.: Substantial nitrogen oxides emission reduction from China due to COVID-19 and its impact on surface ozone and aerosol pollution, Sci. Total. Environ., 753, 142238, 10.1016/j.scitotenv.2020.142238, 2021.

Zhang, R., Zhang, Y., Lin, H., Feng, X., Fu, T.-M., and Wang, Y.: NO_x Emission Reduction and Recovery during COVID-19 in East China, Atmosphere, 11, 10.3390/atmos11040433, 2020.

Zhao, B., Wang, S. X., Liu, H., Xu, J. Y., Fu, K., Klimont, Z., Hao, J. M., He, K. B., Cofala, J., and Amann, M.: NO_x emissions in China: historical trends and future perspectives, Atmos. Chem. Phys., 13, 9869-9897, 10.5194/acp-13-9869-2013, 2013.

Zhao, B., Zheng, H., Wang, S., Smith, K. R., Lu, X., Aunan, K., Gu, Y., Wang, Y., Ding, D., Xing, J., Fu, X., Yang, X., Liou, K. N., and Hao, J.: Change in household fuels dominates the decrease in $PM_{2.5}$ exposure and premature mortality in China in 2005-2015, Proc. Natl. Acad. Sci. USA, 115, 12401-12406, 10.1073/pnas.1812955115, 2018.

Zhao, X., Zhou, W., and Han, L.: Human activities and urban air pollution in Chinese mega city: An insight of ozone weekend effect in Beijing, Phys. Chem. Earth, 110, 109-116, 10.1016/j.pce.2018.11.005, 2019.

Zheng, B., Zhang, Q., Geng, G., Shi, Q., Lei, Y., and He, K.: Changes in China's anthropogenic emissions during the COVID-19 pandemic [data set], figshare, Collection, https://doi.org/10.6084/m9.figshare.c.5214920.v2, 2021a.

Zheng, B., Chevallier, F., Ciais, P., Broquet, G., Wang, Y., Lian, J., and Zhao, Y.: Observing carbon dioxide emissions over China's cities and industrial areas with the Orbiting Carbon Observatory-2, Atmos. Chem. Phys., 20, 8501-8510, 10.5194/acp-20-8501-2020, 2020a.

Zheng, B., Zhang, Q., Geng, G., Chen, C., Shi, Q., Cui, M., Lei, Y., and He, K.: Changes in China's anthropogenic emissions and air quality during the COVID-19 pandemic in 2020, Earth Syst. Sci. Data, 13, 2895-2907, 10.5194/essd-13-2895-2021, 2021b.

Zheng, B., Geng, G., Ciais, P., Davis, S. J., Martin, R. V., Meng, J., Wu, N., Chevallier, F., Broquet, G., Boersma, F., van der A, R. J., Lin, J., Guan, D., Lei, Y., He, K., and Zhang, Q.: Satelite-based estimats of decline and rebound in China's CO_2 emissions during COVID-19 pandemic, Sci. Adv., 6, eabd4998, 2020b.

Zheng, B., Geng, G., Ciais, P., Davis, S. J., Martin, R. V., Meng, J., Wu, N., Chevallier, F., Broquet, G., Boersma, F., van der, A. R., Lin, J., Guan, D., Lei, Y., He, K., and Zhang, Q.: Satellite-based estimates of decline and rebound in China's CO_2 emissions during COVID-19 pandemic, Sci. Adv., 6, 10.1126/sciadv.abd4998, 2020c.

Zheng, H., Zhao, B., Wang, S., Wang, T., Ding, D., Chang, X., Liu, K., Xing, J., Dong, Z., Aunan, K., Liu, T., Wu, X., Zhang, S., and Wu, Y.: Transition in source contributions of $PM_{2.5}$ exposure and associated premature mortality in China during 2005-2015, Environ. Int., 132, 105111, 10.1016/j.envint.2019.105111, 2019.